crystals

MDPI

Article

Field-Induced Transition in $(Nd,Dy)_2Fe_{14}B$ in Ultrahigh Magnetic Fields

N. V. Kostyuchenko [1,*], I. S. Tereshina [2], A. I. Bykov [3], S. V. Galanova [3], R. V. Kozabaranov [3,4], A. S. Korshunov [3], I. S. Strelkov [3], I. V. Makarov [3], A. V. Filippov [3], Yu. B. Kudasov [3,4], D. A. Maslov [3,4], V. V. Platonov [3,4], O. M. Surdin [3,4], P. B. Repin [3], V. D. Selemir [3,4] and A. K. Zvezdin [5,6]

[1] Moscow Institute of Physics and Technology, National Research University, Dolgoprudny, 141701 Moscow, Russia
[2] Faculty of Physics, Lomonosov Moscow State University, 119234 Moscow, Russia
[3] Russian Federal Nuclear Center—VNIIEF, 607188 Sarov, Russia
[4] Sarov Physics and Technology Institute NRNU MEPhI, 607188 Sarov, Russia
[5] Prokhorov General Physics Institute of the Russian Academy of Sciences, 119991 Moscow, Russia
[6] P. N. Lebedev Physical Institute of the Russian Academy of Sciences, 119991 Moscow, Russia
* Correspondence: nvkost@gmail.com

Abstract: We demonstrate the peculiarities of the magnetization process in the ferrimagnetic intermetallic compound $(Nd_{0.5}Dy_{0.5})_2Fe_{14}B$, which has been studied theoretically and experimentally using ultrahigh magnetic fields. We observe phase transition induced by external ultrahigh magnetic fields (up to 170 T) and also describe the magnetization process analytically in terms of critical transition fields. In this work, the first and second critical fields of the field-induced magnetic transitions, H_{c1} and H_{c2}, were estimated, and the results were verified against experimental data for H_{c1}. Critical field H_{c2} predicting the place of transition to the forced-ferromagnetic state was estimated for the first time for $(Nd_{0.5}Dy_{0.5})_2Fe_{14}B$ compound. A comparison of the magnetization behavior for $(Nd_{0.5}Dy_{0.5})_2Fe_{14}B$ with the basic systems $Nd_2Fe_{14}B$ and $Dy_2Fe_{14}B$ is also performed. We demonstrate that, in the $Dy_2Fe_{14}B$ compound, the field-induced transition type is changed from the first to the second order due to the replacement of the Nd atom by Dy one.

Keywords: complex modified materials; critical fields; exchange coupling; hard magnetic materials; ultrahigh magnetic fields; R–Fe exchange; rare-earth intermetallics

Citation: Kostyuchenko, N.V.; Tereshina, I.S.; Bykov, A.I.; Galanova, S.V.; Kozabaranov, R.V.; Korshunov, A.S.; Strelkov, I.S.; Makarov, I.V.; Filippov, A.V.; Kudasov, Y.B.; et al. Field-Induced Transition in $(Nd,Dy)_2Fe_{14}B$ in Ultrahigh Magnetic Fields. *Crystals* **2022**, *12*, 1615. https://doi.org/10.3390/cryst12111615

Academic Editor: Xiaoguan Zhang

Received: 26 October 2022
Accepted: 8 November 2022
Published: 11 November 2022

1. Introduction

In the last few decades, searching for new materials for high-performance permanent magnets is an overriding task for modern physicists and technologists as these magnets are key driving components for electric motors, wind turbines, mobile phones, magnetic memory, and several other products [1–3].

Curie temperature T_c, magnetic anisotropy constant K, and saturation magnetization M_s of such materials are fundamental characteristics used to classify the existing permanent magnets. At Curie temperature, a material loses its ferromagnetic properties; hence, the higher the T_c, the better are the magnets to be used under extreme conditions. High values of saturation magnetization and magnetic anisotropy constants contribute to the creation of high-coercivity magnets that are very important for different practical applications [4–8].

Scientists pay the greatest attention to intermetallic compounds based on rare earth metals (R) and iron, in the fundamental magnetic properties, including exchange interaction parameters of R-Fe compounds, which can be studied most effectively by magnetization measurements in high magnetic fields. Ferrimagnetically ordered compounds are the most interesting because the ferrimagnetic structure is affected by applied external magnetic field, and a sequence of spin–reorientation phase transitions can be observed until the compound reaches magnetic saturation. In order to achieve the full magnetic saturation and

to maintain the compound in the forced-ferromagnetic state, the ultrahigh magnetic fields are required [9–12]. In addition, interest of magnetic phase transitions study in $(R,R')_2Fe_{14}B$ compounds is increasing due to the recent discovery of skyrmions in $Nd_2Fe_{14}B$ [13].

Obtaining high and ultrahigh fields, as well as obtaining reliable experimental data on the magnetization of samples, is a technically difficult task, which is the subject of great efforts of scientists from different countries as a rule. Generation of magnetic fields involves having an electric current flow through a coil, and the field intensity B is proportional to the current I. The heat dissipation I^2R is proportional to the square of the magnetic field, where R is the coil's resistance. The mechanical pressure is also proportional to B^2, with a proportionality coefficient of approximately 4 atm/T^2. Heating and mechanical forces are the two essential problems for the generation of high fields. The stored energy in magnetic field depends on the volume of the magnet, so the size of the field volume is also an important characteristic of the magnet. Another key parameter is whether a magnet is DC or pulsed and, in the latter case, additional important parameters are the duration, temporal profile of the pulse, and the pulse repetition rate. There are several different approaches to overcome the heat–dissipation and mechanical-stability challenges, which is demonstrated in Figure 1 [14]. In all cases, choice of materials is crucially important, so such development is a task at the intersection of physics, engineering, and materials sciences.

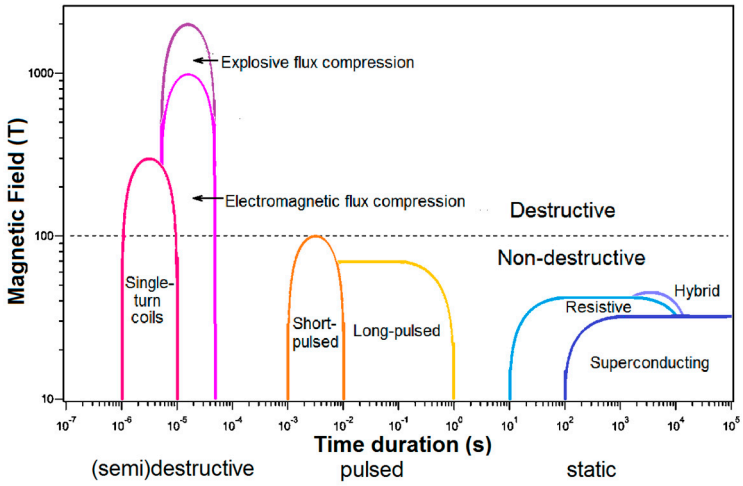

Figure 1. Overview of methods for obtaining high and ultrahigh magnetic fields [14].

It should be noted that the highest-field magnet is not necessarily the best choice for a particular experiment. The figure-of-merit (FOM), depending on the experiment, could be the stored energy B^2V (where V is the field volume), or the effective B^2L (where L is the length of the field), or something else such as the tunability to a desired field value, or the broad operating range of the field values while keeping spatial homogeneity.

There are several laboratories around the world that conduct generation and research of high magnetic fields: the French Laboratoire National des Champs Magnetiques Intenses (LNCMI) with two locations; the German Dresden High Magnetic Field Laboratory (Hochfeld-Magnetlabor Dresden, HLD); and the High Field Magnet Laboratory (HMFL) in the Netherlands. These laboratories operate within the European Magnetic Field Laboratory (EMFL). The US National High Magnetic Field Laboratory (NHMFL) also has three locations. There are two laboratories in China: the High Magnetic Field Laboratory of the Chinese Academy of Sciences (CHMFL) and the Wuhan National High Magnetic Field Center (WHMFC), and four laboratories in Japan: the Tsukuba Magnet Laboratory (TML), the High Field Laboratory for Superconducting Materials, the International Megagauss Science Laboratory (IMGSL), and the Center for Advanced High Magnetic Field Science.

In our work, magnetization measurements were carried out at the Russian Federal Nuclear Center in Sarov in pulsed magnetic fields up to 170 T. This laboratory was one of the first in the world to obtain megagauss magnetic fields [15]. As the object of our

study, we used the composition $(Nd_{0.5}Dy_{0.5})_2Fe_{14}B$, which, due to the Dy atoms, is a ferrimagnet. Previously, this composition was studied by us in magnetic fields up to 58 T at the Dresden High Magnetic Field Laboratory. The experiment showed that the fields used were not enough to observe the forced-ferromagnetic state but allowed us to discuss the transition to the non-collinear phase and make a prediction about the place of the transition in a forced-ferromagnetic state. In addition, at the Megagauss Laboratory of Institute for Solid State Physics of University of Tokyo, the transition from a collinear ferrimagnet and a non-collinear spin-flop-like phase was observed in the $Dy_2Fe_{14}B$ compound in magnetic fields up to 120 T [16]. It was also shown that such studies make it possible to compare the obtained experimental data with existing modern theoretical models and obtain the most important information about the main fundamental parameters for the $(Nd,Dy)_2Fe_{14}B$ compound.

2. Materials and Methods

2.1. Sample Preparation

The samples for this study $(Nd_xDy_{1-x})_2Fe_{14}B$ with x = 0, 0.5 and 1 were prepared using an arc furnace. The procedure for the samples obtaining is described in more details in the following works [17,18]. The phase composition of the samples was determined using the standard X-ray powder diffraction (XRD) at room temperature. XRD studies indicated that the $Nd_2Fe_{14}B$ and $Dy_2Fe_{14}B$ alloys were single-phase, while, in the $(Nd,Dy)_2Fe_{14}B$ samples, traces of the second phase were seen (~5%). The investigated alloys have a tetragonal structure of the $Nd_2Fe_{14}B$ type (space group P42/mnm) at room temperature. The lattice parameters for $Nd_2Fe_{14}B$, $(Nd_xDy_{1-x})_2Fe_{14}B$ and $Dy_2Fe_{14}B$ alloys are a = 0.880 nm, c = 1.219 nm, a = 0.877 nm, c = 1.212 nm, a = 0.873 nm, and c = 1.190 nm, respectively. The decreasing lattice parameter for the Dy-substituted compound is due to the smaller atomic radius of Dy^{3+} as compared to Nd^{3+}. This agrees well with literature data [16].

2.2. Method of Magnetization Measurements

Magnetization measurements were performed at the Russian Federal Nuclear Center in Sarov in pulsed magnetic fields up to 170 T on powder samples. An ultrahigh magnetic field up to 600 T was created in a magnetocumulative generator MC-1 [19]. In a thin-walled wire solenoid, the discharge of a powerful capacitor bank with a stored energy of 2 MJ created a seed magnetic field of about 16 T. During the battery discharge, a converging shock wave was initiated in the annular charge of high explosives surrounding the solenoid. It came out on the surface of the solenoid at the seed field maximum (approximately 80 μs after the start of the discharge). When the shock wave passed through the solenoid, the solenoid wires were welded and formed a homogeneous conducting cylinder shell with the trapped magnetic flux. The ultrahigh magnetic field was generated by explosive magnetic flux compression for about 16 μs. The MC-1 generator has been widely used earlier and proved to be a reliable tool for scientific research [20]. The high uniformity of the magnetic field in large useful volumes (about 10 cm^3) made it possible to install four researched samples in one experiment.

2.3. Registration of the Signal

The registration of the time derivative of the magnetic field was carried out by a set of pick-up coils with different sensitivities (7 coils in total, some of them were duplicated to increase reliability). It allowed measurements of the magnetic field induction with an accuracy of 5% over the entire operating range of the MC-1 generator. The magnetization of the studied samples was measured using compensated pick-up coils [21,22]. A pair of two identical coils were of diameter d = 2.8 mm and had number of turns N = 20. A special winding of the sensor was performed, which provided a significant reduction of the total electrical voltage between the coils of the sensor [21]. The signal induced in the compensation coils consists of a "useful" part and background signal, which stemmed from the coil decompensation and was proportional to the time derivative of the magnetic

field. The degree of decompensation for all sensors was less than 2%. To take into account a slight attenuation of the signals of the compensation sensors in cable lines, the whole system was pre-calibrated immediately before the experiment. The compensated pick-up coils were proven to be a reliable technique for magnetization measurements at pulsed magnetic fields [20–22]. The compensation sensors were placed in a glass helium cryostat, into which liquid helium was raised from a transport Dewar vessel before the experiment.

The absolute values of the magnetization were calibrated by measuring the magnetization curves up to 14 T in static fields using a PPMS 14T magnetometer (Quantum Design, San Diego, CA, USA).

3. Results

Figure 2 displays the magnetization curves of the $Dy_2Fe_{14}B$ and $Nd_2Fe_{14}B$ single crystals measured at 1.8 and 10 K, respectively. Measurements have been performed along the main crystallographic axes and compared with the data given in the works [18,23]. $Nd_2Fe_{14}B$ samples display an easy-cone anisotropy, in contrast to the uniaxial $Dy_2Fe_{14}B$ with an anisotropy field of 27 T. In the inset in Figure 2, we show the magnetization curve of aligned polycrystal sample $Dy_2Fe_{14}B$ in magnetic fields up to 120 T obtained at 10 K [16]. The anomaly near 100 T (at 105 and 101 T for increasing and decreasing fields, respectively, which correspond to intermittent changes in the M(H) curve) arises from the first-order transition between a collinear ferrimagnet and a non-collinear spin-flop-like phase. In the $Nd_2Fe_{14}B$ single crystal, a jump in the M(H) magnetization curve is observed along the [100] direction in magnetic field 17 T.

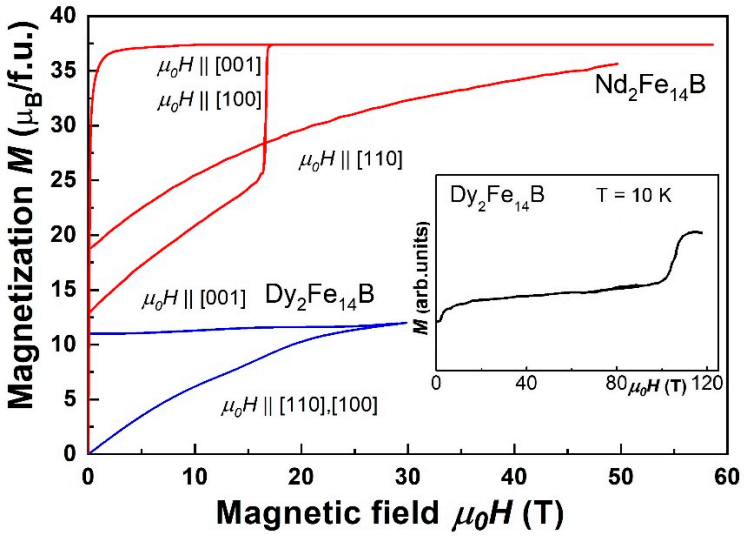

Figure 2. Magnetization curves of $Dy_2Fe_{14}B$ and $Nd_2Fe_{14}B$ single crystals applied along the main crystallographic directions at 1.8 and 10 K, respectively [18,23]. Inset: The data for an aligned polycrystal $Dy_2Fe_{14}B$ at 10 K (for increasing fields [16]) are shown for comparison.

Figure 3 demonstrates the magnetization curves of the $(Nd_{0.5}Dy_{0.5})_2Fe_{14}B$ compound along the perpendicular [001] easy axis. Magnetization measurements were performed by us at the Dresden High Magnetic Field Laboratory in pulsed magnetic fields up to 58 T previously [18]. The measurements up to 170 T obtained for the first time at the Russian Federal Nuclear Center in Sarov. It should be mentioned that a compensated pick-up sensor, in fact, measured a time derivative of magnetization. This is why the flat segments of the magnetization curve in Figure 3 were beyond the sensitivity and shown by the dashed line. A partial substitution of Dy by Nd atom in the latter compound results in an increase of the anisotropy field where the easy- and hard-axis magnetization curves intersect. Such new results, containing features on the magnetization curve, can also be used for modern

numerical calculations, including for obtaining or refining the exchange and crystal-field parameters in the quantum model of the crystal electric field [16–18].

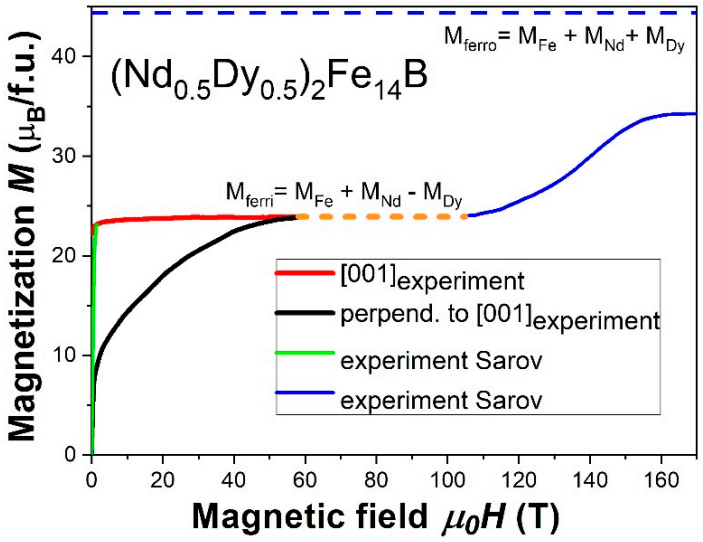

Figure 3. Magnetization curves of $(Nd_{0.5}Dy_{0.5})_2Fe_{14}B$ at 1.8 K in magnetic fields up to 58 T applied along the perpendicular easy axis c (red and black lines) [18] and at 4.2 K in fields up to 170 T (for increasing fields) applied along the c-axis (green and blue lines).

Figure 3 shows that the experimental data obtained in different laboratories are in good agreement with each other. Moreover, it can be stated that ultrahigh magnetic fields in the $(Nd_{0.5}Dy_{0.5})_2Fe_{14}B$ compound induce a magnetic phase transition similar to that observed earlier in the $Dy_2Fe_{14}B$ compound. These transitions can be interpreted as intermediate processes from ferrimagnetism to forced ferromagnetism. A significant difference here is the fact that the magnetic phase transition in the substituted composition $(Nd_{0.5}Dy_{0.5})_2Fe_{14}B$ occurs smoothly, covering a quite large range of magnetic fields from 105 T to 160 T, exhibiting features characteristic of second-order phase transitions.

4. Discussion

In order to analyze obtained experimental data, it is important to understand which sections of the magnetization curves correspond to which phase: ferrimagnetic, non-collinear, or ferromagnetic (field-induced forced ferromagnetic state). This can be understood using a quite simple analytical approach in terms of the first and second critical fields. The first critical field H_{c1} corresponds to the transition from the ferrimagnetic to the non-collinear phase, and the second H_{c2} to the ferromagnetic one. In order to estimate them, we applied the analytical approach (previously described in detail in Refs. [24–27]) well proven for the $(R,R')_2Fe_{14}B$ intermetallic compounds.

For the $R_2Fe_{14}B$ compounds, both critical fields H_{c1} and H_{c2} are equal to [24,26,27]:

$$\begin{aligned} H_{c1} &= \lambda\,(M_{Fe} - 2M_R) + \frac{H_a\,2M_R}{\lambda\,(M_{Fe} - 2M_R)}, \\ H_{c2} &= \lambda\,(M_{Fe} + 2M_R) - \frac{H_a\,2M_R}{\lambda\,(M_{Fe} + 2M_R)} \end{aligned} \quad (1)$$

where λ is the R-Fe intersublattice exchange parameter, $H_a = \frac{2K_1}{M_{Fe}}$ is the magnetic anisotropy field, and K_1 is magnetic anisotropy constant [5]. Here, the second term describing the anisotropy has been added in order to make a more accurate critical fields estimation [27]. Thus, the accuracy of analytical evaluations of the critical fields reaches several Tesla.

For the $(Nd_{0.5}Dy_{0.5})_2Fe_{14}B$ compound with two different rare-earth ions, the critical fields H_{c1} and H_{c2} have the form [27]

$$\begin{aligned} H_{c1} &= \lambda_{Dy}\left(M_{Fe} - 2M_{Dy}\xi_1\right) - \frac{2M_{Dy}H_a\xi_1^2}{\left(M_{Fe}-2M_{Dy}\xi_1\right)}, \\ H_{c2} &= \lambda_{Dy}\left(M_{Fe} + 2M_{Dy}\xi_2\right) + \frac{2M_{Dy}H_a\xi_2^2}{\left(M_{Fe}+2M_{Dy}\xi_2\right)}, \\ \xi_i(H_{ci}) &= \frac{1}{1+\lambda_{Nd}\chi_{Nd}(H_{ci})};\ \chi_{Nd}(H_{ci}) = \frac{2M_{Nd}}{\lambda_{Nd}M_{Fe}+H_{ci}}; i = 1,2 \end{aligned} \quad (2)$$

λ_{Nd} and χ_{Nd} are the exchange parameter and susceptibility of the Nd sublattice, respectively. In accordance with our previous estimates, $\xi_i \approx 0.9$ [24]. Formula (2) with anisotropic correction is universal and could be used for various rare-earth intermetallics. H_{c1} and H_{c2} values obtained for $(Nd_{0.5}Dy_{0.5})_2Fe_{14}B$ and $Dy_2Fe_{14}B$ by analyzing high-field experimental data using Formulas (1) and (2) are given in Table 1.

Table 1. Magnetic critical fields' parameters H_{c1} and H_{c2} for $(Nd_{0.5}Dy_{0.5})_2Fe_{14}B$ and $Dy_2Fe_{14}B$.

Compound	H_{c1} (T)	H_{c2} (T)
$(Nd_{0.5}Dy_{0.5})_2Fe_{14}B$	105	240
$Dy_2Fe_{14}B$	105	250

H_{c2} value provides important information, which the magnitudes of external magnetic fields require to reach the ferromagnetic state, and allow us to plan new ultrahigh magnetization experiments for studying similar types of compounds. It can be seen that, in order to experimentally observe the transition to the forced-ferromagnetic phase, both compounds ($(Nd_{0.5}Dy_{0.5})_2Fe_{14}B$ and $Dy_2Fe_{14}B$) require magnetic fields greater than 250 T. This is confirmed, among other things, by the value of the magnetization in the $(Nd_{0.5}Dy_{0.5})_2Fe_{14}B$ compound at 170 T. It reaches magnitude 34 μ_B/f.u., while the magnitude of the magnetization in a forced-ferromagnetic state is 44.1 μ_B/f.u. (see Table 2), that is, in the magnetic field 170 T, saturation has not yet been obtained.

Table 2. Values of the rare-earth and iron magnetic moments for $(Nd_{0.5}Dy_{0.5})_2Fe_{14}B$ and $Dy_2Fe_{14}B$ intermetallic compounds.

Compound	M_{Fe} (μ_B)	M_R (μ_B)
$(Nd_{0.5}Dy_{0.5})_2Fe_{14}B$	31.4	3 (Nd) and 10 (Dy)
$Dy_2Fe_{14}B$	31.4	10

5. Conclusions

Magnetization measurements were performed for the intermetallic ferrimagnetic compound $(Nd_{0.5}Dy_{0.5})_2Fe_{14}B$ using ultrahigh magnetic fields up to 170 T. Such high magnetic fields make it possible to observe the experimentally field-induced phase transition from the initial ferrimagnetic state to the non-collinear one. The results obtained were compared with the literature high-field magnetization data for the basic $Dy_2Fe_{14}B$ compound. We have determined two critical fields (H_{c1} and H_{c2}) of field-induced transitions for the compounds under study. We demonstrate that, in order to observe the transition to the forced-ferromagnetic state, both compounds ($(Nd_{0.5}Dy_{0.5})_2Fe_{14}B$ and $Dy_2Fe_{14}B$) require magnetic fields greater than 250 T. It is shown that the replacement of one rare-earth atom by another is a powerful tool for controlling the properties of rare-earth $R_2Fe_{14}B$-type compounds, on the basis of which modern highly efficient permanent magnets are manufactured.

Author Contributions: Methodology, Y.B.K., D.A.M., V.V.P. and O.M.S.; investigation, N.V.K., A.K.Z., A.I.B., S.V.G., R.V.K., A.S.K., I.S.S., I.V.M. and A.V.F.; writing—original draft preparation, N.V.K.; writing—review and editing, I.S.T. and Y.B.K.; supervision, I.S.T. and Y.B.K.; project administration, A.K.Z., P.B.R. and V.D.S. All authors have read and agreed to the published version of the manuscript.

Funding: This work was supported by the Ministry of Science and Higher Education of the Russian Federation (No. FSMG-2021-0005). Research in ultrahigh magnetic fields was carried out within the framework of the scientific program of the National Center for Physics and Mathematics (Project "Research in high and ultrahigh magnetic fields").

Institutional Review Board Statement: Not applicable.

Informed Consent Statement: Not applicable.

Data Availability Statement: Not applicable.

Conflicts of Interest: The authors declare no conflict of interest.

References

1. Kostyuchenko, N.V.; Tereshina, I.S.; Andreev, A.V.; Doerr, M.; Tereshina-Chitrova, E.A.; Paukov, M.A.; Gorbunov, D.I.; Politova, G.A.; Pyatakov, A.P.; Miyata, A.; et al. Investigation of the field-induced phase transitions in the (R, R′)$_2$Fe$_{14}$B rare-earth intermetallics in ultra-high magnetic fields. *IEEE Trans. Magn.* **2021**, *57*, 2101105. [CrossRef]
2. Coey, J.M.D. Hard Magnetic Materials: A Perspective. *IEEE Trans. Magn.* **2011**, *47*, 4671–4681. [CrossRef]
3. Coey, J.M.D. Perspective and Prospects for Rare Earth Permanent Magnets. *Engineering* **2020**, *6*, 119–131. [CrossRef]
4. Gutfleisch, O.; Willard, M.A.; Brück, E.; Chen, C.H.; Sankar, S.G.; Liu, J.P. Magnetic Materials and Devices for the 21st Century: Stronger, Lighter, and More Energy Efficient. *Adv. Mater.* **2011**, *23*, 821–842. [CrossRef] [PubMed]
5. Sepehri-Amin, H.; Hirosawa, S.; Hono, K. Chapter 4—Advances in Nd-Fe-B Based Permanent Magnets. In *Handbook of Magnetic Materials*; Elsevier: Amsterdam, The Netherlands, 2018; Volume 27, pp. 269–372.
6. Herbst, J.F. R$_2$Fe$_{14}$B materials: Intrinsic properties and technological aspects. *Rev. Mod. Phys.* **1991**, *63*, 819–898. [CrossRef]
7. Li, H.-S.; Coey, J.M.D. Chapter 3—Magnetic properties of ternary rare-earth transition-metal compounds. In *Handbook of Magnetic Materials*; Elsevier: Amsterdam, The Netherlands, 2019; Volume 28, pp. 87–196.
8. Gabay, A.M.; Marinescu, M.; Li, W.F.; Liu, J.F.; Hadjipanayis, G.C. Dysprosium-saving improvement of coercivity in Nd-Fe-B sintered magnets by Dy_2S_3 additions. *J. Appl. Phys.* **2011**, *109*, 083916. [CrossRef]
9. Liu, W.-Q.; Chang, C.; Yue, M.; Yang, J.-S.; Zhang, D.-T.; Zhang, J.-X.; Liu, Y.-Q. Coercivity, microstructure, and thermal stability of sintered Nd–Fe–B magnets by grain boundary diffusion with TbH_3 nanoparticles. *Rare Met.* **2017**, *36*, 718–722. [CrossRef]
10. Poenaru, I.; Lixandru, A.; Güth, K.; Malfliet, A.; Yoon, S.; Škulj, I.; Gutfleisch, O. HDDR treatment of Ce-substituted Nd$_2$Fe$_{14}$B-based permanent magnet alloys—Phase structure evolution, intergranular processes and magnetic property development. *J. Alloys Compd.* **2020**, *814*, 152215. [CrossRef]
11. Sözen, H.İ.; Ener, S.; Maccari, F.; Skokov, K.P.; Gutfleisch, O.; Körmann, F.; Neugebauer, J.; Hickel, T. Ab initio phase stabilities of Ce-based hard magnetic materials and comparison with experimental phase diagrams. *Phys. Rev. Mater.* **2019**, *3*, 084407. [CrossRef]
12. Furlani, E.P. *Permanent Magnet and Electromechanical Devices: Materials, Analysis, and Applications*; Academic Press: Cambridge, MA, USA, 2001.
13. Chaboy, J.; Piquer, C.; Plugaru, N.; Bartolomé, F.; Laguna-Marco, M.A.; Plazaola, F. ^{57}Fe Mössbauer and x-ray magnetic circular dichroism study of magnetic compensation of the rare-earth sublattice in $Nd_{2-x}Ho_xFe_{14}B$ compounds. *Phys. Rev. B* **2007**, *76*, 134408. [CrossRef]
14. Xiao, Y.; Morvan, F.J.; He, A.N.; Wang, M.K.; Luo, H.B.; Jiao, R.B.; Xia, W.X.; Zhao, G.P.; Liu, J.P. Spin-reorientation transition induced magnetic skyrmion in Nd$_2$Fe$_{14}$B magnet. *Appl. Phys. Lett.* **2020**, *117*, 132402. [CrossRef]
15. Battesti, R.; Beard, J.; Böser, S.; Bruyant, N.; Budker, D.; Crooker, S.A.; Daw, E.J.; Flambaum, V.V.; Inada, T.; Irastorza, I.G.; et al. High magnetic fields for fundamental physics. *Phys. Rep.* **2018**, *765*, 1–39. [CrossRef]
16. Younger, S.; Lindemuth, I.; Reinovsky, R.; Fowler, C.M.; Goforth, J.; Ekdahl, C. Scientific Collaborations Between Los Alamos and Arzamas-16 Using Explosive-Driven Flux Compression Generators. *Los Alamos Sci.* **1996**, *24*, 48–67.
17. Lim, D.W.; Kato, H.; Yamada, M.; Kido, G.; Nakagawa, Y. High-field magnetization process and spin reorientation in $(Nd_{1-x}Dy_x)_2Fe_{14}B$ single crystals. *Phys. Rev. B* **1991**, *44*, 10014. [CrossRef] [PubMed]
18. Takeyama, S.; Amaya, K.; Nakagawa, T.; Ishizuka, M.; Nakao, K.; Sakakibara, T.; Goto, T.; Miura, N.; Ajiro, Y.; Kikuchi, H. Magnetisation measurements in ultra-high magnetic fields produced by a single-turn coil system. *J. Phys. E Sci. Instrum.* **1988**, *21*, 1025. [CrossRef]
19. Kostyuchenko, N.V.; Tereshina, I.S.; Gorbunov, D.I.; Tereshina-Chitrova, E.A.; Andreev, A.V.; Doerr, M.; Politova, G.A.; Zvezdin, A.K. Features of magnetization behavior in the rare-earth intermetallic compound $(Nd_{0.5}Ho_{0.5})_2Fe_{14}B$. *Intermetallics* **2018**, *98*, 139–142. [CrossRef]

20. Shneerson, G.A.; Dolotenko, M.I.; Krivosheev, S.I. *Strong and Superstrong Magnetic Fields Generation*; Walter de Gruter GmbH: Berlin, Germany, 2014.
21. Boriskov, G.V.; Bykov, A.I.; Dolotenko, M.I.; Egorov, N.I.; Kudasov, Y.B.; Platonov, V.V.; Selemir, V.D.; Tatsenko, O.M. Research in ultrahigh magnetic field physics. *Phys. Uspekhi* **2011**, *54*, 421–427. [CrossRef]
22. Kudasov, Y.B. Megagauss magnetization measurements. *Phys. B Condens. Matter* **2001**, *294*, 684–690. [CrossRef]
23. Kostyuchenko, N.V.; Tereshina, I.S.; Gorbunov, D.I.; Tereshina-Chitrova, E.A.; Rogacki, K.; Andreev, A.V.; Doerr, M.; Politova, G.A.; Zvezdin, A.K. High-field magnetization study of $(Nd,Dy)_2Fe_{14}B$: Intrinsic properties and promising compositions. *Intermetallics* **2020**, *124*, 106840. [CrossRef]
24. Eslava, G.G.; Fayyazi, B.; Skokov, K.; Skourski, Y.; Gorbunov, D.; Gutfleisch, O.; Dempsey, N.M.; Givord, D. A two-sublattice model for extracting rare-earth anisotropy constants from measurements on $(Nd,Ce)_2(Fe,Co)_{14}B$ single crystals. *J. Magn. Magn. Mater.* **2021**, *520*, 167470. [CrossRef]
25. Tereshina, I.S.; Pyatakov, A.P.; Tereshina-Chitrova, E.A.; Gorbunov, D.I.; Skourski, Y.; Law, J.M.; Paukov, M.A.; Havela, L.; Doerr, M.; Zvezdin, A.K.; et al. Probing the exchange coupling in the complex modified Ho-Fe-B compounds by high-field magnetization measurements. *AIP Adv.* **2018**, *8*, 125223. [CrossRef]
26. Zvezdin, A.K.; Lubashevskii, I.A.; Levitin, R.Z.; Platonov, V.V.; Tatsenko, O.M. Phase transitions in megagauss magnetic fields. *Phys. Uspekhi* **1998**, *41*, 1037–1042. [CrossRef]
27. Zvezdin, A.K. Magnetic Phase Transitions: Field-induced (Order-to-order). In *Encyclopedia of Materials: Science and Technology*; Buschow, K.H.J., Cahn, R.W., Flemings, M.C., Ilschner, B., Kramer, E.J., Mahajan, S., Veyssière, P., Eds.; Elsevier: Amsterdam, The Netherlands, 2001; pp. 4841–4847.